Five Years Of Recording VLF Intensities In Inner Plasmasphere Using C/NOFS VEFI

Abram Jacobson[1] and Robert Holzworth[1]

[1]University of Washington

November 24, 2022

Abstract

The Vector Electric Field Instrument (VEFI) aboard the CNOFS satellite recorded over 20 thousand 12-s-duration, 3-axis continuous VLF waveforms syncronously on 3 crossed antenna booms. Tbis provides an important data archive on Poynting flux and wave intensity, of relevance to wave-particle interactions in tbe low-latitude inner plasmasphere. We will provide a summary of all the observations, not limited to discrete whistlers associable with known lightning events (our focus in previous reports).

SM33C-3598 Five Years Of Recording VLF Intensities In Inner Plasmasphere Using C/NOFS VEFI

Abram Jacobson* and Robert Holzworth, University of Washington; Robert Pfaff, NASA Goddard; Roderick Heelis, University of Texas Dallas ***corresponding author: abramj@u.washington.edu**

Work supported in part by NSF project 1443011

Bibliography

The following articles describe prior work we have done with C/NOFS:

Heelis, R. A., W. R. Coley, A. G. Burrell, M. R. Hairston, G. D. Earle, M. D. Perdue, R. A. Power, L. L. Harmon, B. J. Holt, and C. R. Lippincott (2009), Behavior of the O+/H+ transition height during the extreme solar minimum of 2008, *Geophys. Res. Lett., 36*, L00C03, doi:10.1029/ 2009GL038652, doi:10.1029/ 2009GL038652.

Jacobson , A. R., R. H. Holzworth, R. Pfaff, and R. Heelis (2016), Automated identification of discrete, lightning-generated, multiple-dispersed whistler waves in C/NOFS-VEFI very low frequency observations, *Radio Sci., 51*, doi:10.1002/2016RS005989.

Jacobson, A. R., R. H. Holzworth, R. F. Pfaff, R. Heelis, and P. Colestock (2018), A method to estimate whistler wavevector from polarization using 3-component satellite E-field data, *Radio Sci., 49*, 10.1002/2013RS005335, doi:10.1002/2013RS005335.

Jacobson, A. R., R. H. Holzworth, R. F. Pfaff, and M. F. McCarthy (2011), Study of oblique whistlers in the low-latitude ionosphere, jointly with the C/NOFS satellite and the World-Wide Lightning Location Network, *Annales Geophysicae, 29*, 851-863, doi:10.5194/ angeo-29-851-2011.

Pfaff, R., et al. (2010), Observations of DC electric fields in the low-latitude ionosphere and their variations with local time, longitude, and plasma density during extreme solar minimum, *J. Geophys. Res., 115*, A12324, doi: 10.1029/2010JA016023, doi:10.1029/2010JA016023.

Jacobson , A. R., R. H. Holzworth, R. Pfaff, and R. Heelis (2018), Coordinated Satellite Observations of the Very Low Frequency Transmission Through the Ionospheric D Layer at Low Latitudes, Using Broadband Radio Emissions From Lightning, *Journal of Geophysical Research: Space Physics, 123*, doi:10.1002/2017JA024942.

C/NOFS satellite during 2008 - 2014 was at LEO in low-latitudes (inclination ~ 13 deg), and carried the VEFI (Vector Electric Field Instrument). We used it for 3-axis simultaneous recording of the VLF electric field in the band 0 - 16 kHz. We acquired ~ 20K records, each ~12-sec duration. Of these, 6890 records were both complete (all 3 axes functioning) and high-signal-to-noise ratio, allowing (with CINDI ion composition) precise retrieval of the whistler-wave polarization, index of refraction, and wavevector.

Below is a spectrogram of VLF electric field **E** perpendicular to geomagnetic field. The WWLLN stroke times are shown by green ticks from top axis. The (much fewer) detected narrow whistler 0-hop pulses are shown with longer, orange/pink ticks. Note lower-hybrid scatter at > 11 kHz, and diffuse coda < 7 kHz.

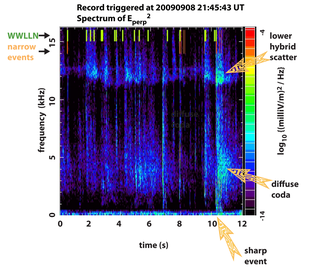

Below is the time-average of the spectrogram from above, restricted to f > 1 kHz. The lower-hybrid frequency (~11 kHz) is shown. Note the enhancement above the lower-hybrid frequency. Nonetheless, most of the power resides in the lower frequencies (< 7 kHz), where occur the diffuse codas. The diffusion of the time signal defeats detection of narrow pulses.

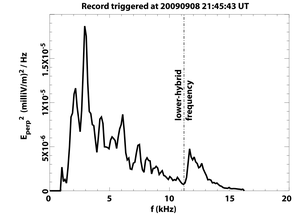

INTRODUCTION

Below is a closer look at the dependence of detected, narrow (<15 samples, or < 0.47 millisec, after automatic dechirping) VLF pulses on magnetic inclination. We use local magnetic inclination as the independent variable, because the modeled D-layer transmission directly and sensitively depends on this angle. (a) The fraction of WWLLN strokes (worldwide) having an identified coincident, narrow VEFI pulse. Each data point is at the centroid of a bin in magnetic inclination. The minimum near the Magnetic Equator (inclination = 0) would seem consistent with the theoretical minimum of D-layer transmission. (b) Logarithm of the bin-median measured transmission, that is, the ratio of the Poynting flux density at VEFI to the modeled Poynting flux density at the subsatellite point, in the Earth-Ionosphere Waveguide. ***This measured transmission ratio's inclination dependence is not consistent with the theoretical expection.***

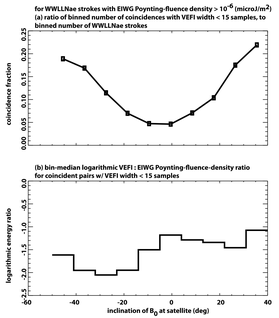

We had assumed when starting this research that the data would show a broad minimum of transmission (through the D-layer) at the Magnetic Equator. The graph (b) to left shows that this is not neatly borne out. ***Below*** is an indicator of the true effect of magnetic inclination on the detectability of VLF pulses arising from lightning. We grade each detected pulse by its width, in digitizer samples (0.031 millisec). We find that pulses wider than 15 samples (0.47 millisec) have diminished likelihood of coincidence with WWLLN lightning strokes. Therefore, for practical applications requiring WWLLN concurrence, we have used only narrow (<15 samples wide) pulses. Below is proof that either (a) the bin-average or (b) the bin-median width increases as the inclination becomes more equatorial, i.e. approaches 0. Black is for abs(inclination) > 25 deg, blue is for 10 to 25 deg, and red is for < 10 deg (very near the Magnetic Equator). ***Pulses transmitted to the satellite are broadened near the Magnetic Equator compared to pulses at higher latitudes.***

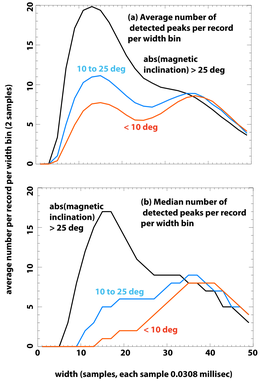

BACKGROUND CONDITIONS

Below is a scatter plot of the positions of all 6890 records used in this study. The position is altitude (vertical axis) versus magnetic inclination (horizontal).

C/NOFS was in a slightly elliptical LEO orbit, inclined ~13 deg, with nominal perigee near 400 km and apogee near 850 km. (During 2014 orbital decay brought it somewhat lower). Each recording is ~ 12-s duration.

The data recordings were made (with only a few exceptions) during local darkness, at quasi-random times over 2008-2014. This began with deep solar minimum, then continued with recovery from minimum. The coverage of altitude/declination was done during this six-year duration and results in partial aliasing amongst solar-flux, altitude, and declination. The purpose of this section is to show the independent variables, and in some cases aliasing amongst them is indicated.

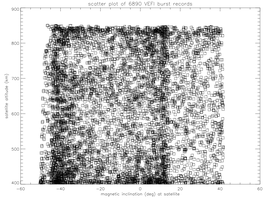

Below is a scatter plot of the positions of all 6890 records used in this study. **Color indicates $\log_{10}$(CINDI ion density, cm^{-3})**, from blue = 3 to red = 5. The cluster of red near -40 deg inclination (lower left corner) is due to concentrated recording late in the mission. The scattered blue-coded records are from recordings near solar minimum.

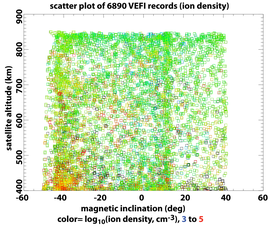

Below is a scatter plot of the positions of all 6890 records used in this study. **Color indicates solar zenith angle at the sub-satellite D-layer**, from blue = 0 to red = 180. Almost all of the records occurred in local darkness. The handful of blue-coded records are from recordings in daylight.

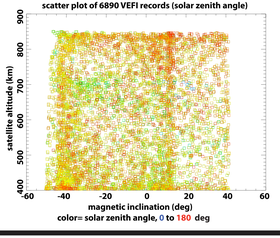

Below is a scatter plot of the positions of all 6890 records used in this study. **Color indicates $\log_{10}$(rms ion-density fluctuations normalized by the sliding mean)**, from blue = -4 to red = -1. Ion-density fluctuations are important, as they are a necessary condition for strongly-developed lower-hybrid scattering.

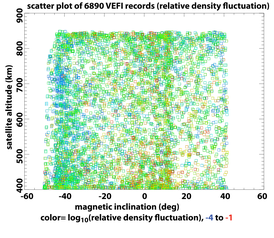

Below is a scatter plot of the positions of all 6890 records used in this study. **Color indicates CINDI oxygen fraction of ions**, from blue = 0 to red = 1. The transition from oxygen-dominated to light-ion-dominated (mainly H$^+$, but some He$^+$) affects both the index of refraction and the lower-hybrid frequency.

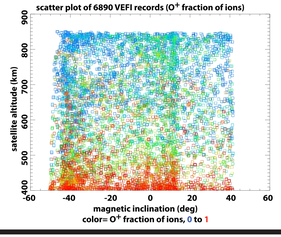

Below is a scatter plot of the positions of all 6890 records used in this study. **Color indicates lower hybrid frequency**, from blue = 0 to red = 18 kHz. Note the obvious aliasing of recording date, that is, when the recording occurred within the varying solar cycle. (Similar to oxygen fraction, previously.)

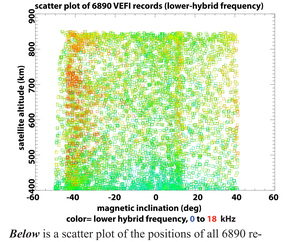

Below is a scatter plot of the positions of all 6890 records used in this study. **Color indicates $\log_{10}$("lower-hybrid enhancement")**, from blue = -3 to red = +2. This is the ratio of the Poynting-flux density in a 2-kHz-wide band above the lower-hybrid frequency, to a similar band below the lower-hybrid frequency. This ratio is ordinarily small (< 0.1) but spikes during pronounced lower-hybrid scattering. particularly near magnetic equator.

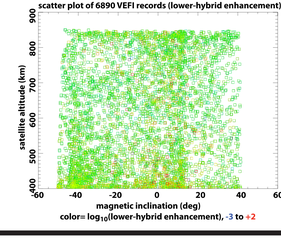

Below is the accumulated distribution of the **lower-hybrid frequency f_{lh}** for all 6890 records. (Same data as shown as color to left.) Note that f_{lh} is usually > 5 kHz, and the mean is around 12 kHz.

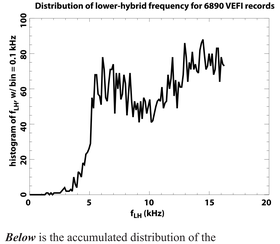

Below is the accumulated distribution of the **$\log_{10}$("lower-hybrid enhancement")** for all 6890 records. This is the ratio of the Poynting-flux density in a 2-kHz-wide band above the lower-hybrid frequency, to a similar band below the lower-hybrid frequency. The vertical dashed line is at 0.3 (so the enhancement ratio there is 2.) This threshold will be used later.

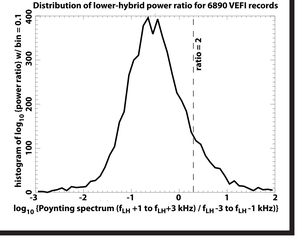

Narrow events vs all power

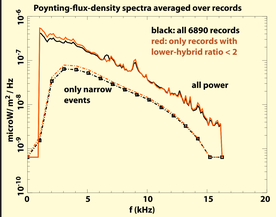

Our previous papers have all focused on the identifed narrow-pulse events that result from automated dechirping of discrete, zero-hop whistler signals. Here we compare the narrow events (dashed curves) with the entirety of the signal (solid curves).
Above: Spectrum of Poynting-flux density, averaged over (black) all 6890 records, and (red) over only those records with lower-hybrid enhancement ratio < 2. The cutoff below 1 kHz is artifially imposed. For f > 5 kHz, narrow events account for only ~25% of the energy. At low frequencies, where the energy peaks, the contribution from narrow events is much smaller. ***Below:*** Distribution of frequency-averaged spectral density of Poynting-flux density, showing that the narrow events account for a minority of the energy.

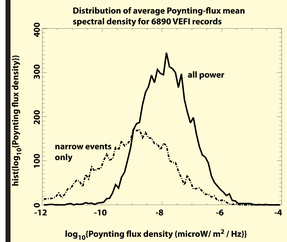

Orientation of wavevector relative to geomagnetic field

We infer the wave polarization, the index of refraction, and the orientation of the wavevector relative to the geomagnetic field, for all pixels in a time-frequency spectrogram of the three-antenna signals. This is based on the Stokes parameters per pixel, plus the concurrent CINDI ion-composition data for the record. The orientation of **k** relative to $\mathbf{B}_0$ is specified by two angles:

1. θ, the polar angle of **k** relative to $\mathbf{B}_0$.

2. τ, the azimuth angle of **k** around $\mathbf{B}_0$. The azimuth is reckoned from magnetic-East-zonal to magnetic-inward-meridional. For example, $\tau = 0$ is magnetic east, $\tau = 90$ is magnetic inward-meridional.

Ducted whistler propagation requires $\theta \sim 0$. By contrast, oblique propagation, which is the only mode available in the absence of ducting, can have any value of θ, all the way to 90 deg.

Below is a Poynting-flux-density-weighted distribution of the angles θ, on the horizontal axis, and τ, on the vertical axis, accumulated over all 6890 records. The distribution is shown separately in three subbands: (a) 1-5 kHz, (b) 5-9 kHz, and (c) 9-15 kHz. ***The power-weighted orientation distribution is strongly oblique and and does not indicate ducted propagation.***
Most of the power maps to **k** nearly within the magnetic meridian, but there is some power associated with **k** not in the meridian, notably at $\tau \sim -50$ deg. The color scale is linear in accumulated Poynting-flux density.

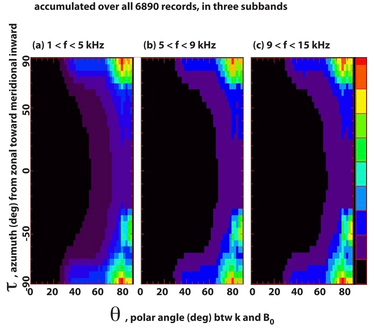

Below is a Poynting-flux-density-weighted distribution of the angles θ, on the horizontal axis, and τ, on the vertical axis, accumulated over all 6890 records. The accumulation is for the band 1-15 kHz. (a) Distribution only for pixels associated with narrow events; (b) distribution for all pixels.
The color scale is linear in accumulated Poynting-flux density.
The (a) narrow events occupy two swarms of oblique **k** solutions, both in the meridian, near $\theta \sim 40$ deg and $\theta \sim 75$ deg. By contrast, (b) the majority power maps to near-orthogonal **k**, with some solutions out of meridian.

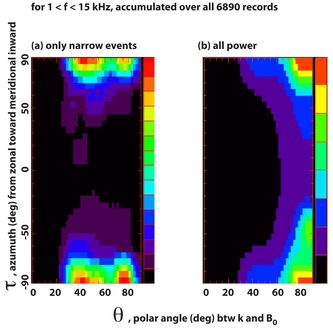

Influence of magnetic inclination on spectral results

To the right are three columns of graphs. On the left is the spectrum of wave E^2. In the center is the spectrum of wave B^2. On the right is the spectrum of Poynting-flux density. The cutoff below 1 kHz is artificially imposed.

Within each column, the top panel is the median spectrum, while the bottom panel is the average spectrum. The average noisily spikes more than the median, and is much larger overall than the median, due to the fact that the average is dominated by a subset of records with extremely active wave records. Put another way, the 6890 records over-estimates the degrees of freedom in these statistics, which in an average sense are dominated by a powerful subset of the 6890 records.

Within each spectrum graph, there are three curves, marked by colors as follows:
Red: abs(magnetic inclination) < 10 deg.
Blue: abs(magnetic inclination) in range 10 to 25 deg.
Black: abs(magnetic inclination) > 25 deg.
Clearly, the spectra near the magnetic equator (red; abs(magnetic inclination) < 10 deg) are the strongest, in all three variables.

This is not consistent with prior expectations based on theory of D-layer transmission's dependence on magnetic inclination. Theory predicts suppressed transmission where $\mathbf{B}_0$ is horizontal.

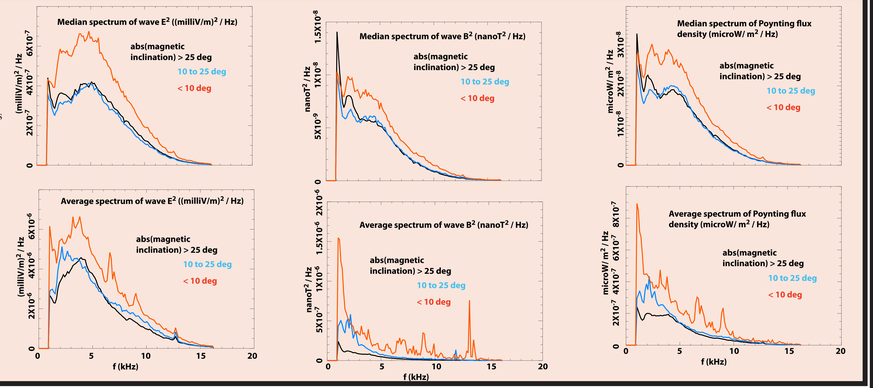

Statistical evidence of whistler energy eroded by lower-hybrid scattering

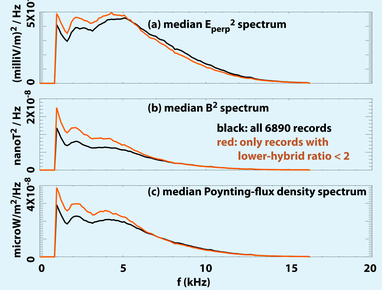

Shown here are median spectra of (a) wave E^2, (b) wave B^2, and (c) Poynting-flux density. The black curves are for medians over all 6890 records, and are identical between the columns on the left and those on the right.

The red curves are for either of two (disjunct) restricted subsets of the records. On the left, the red curves are for lower-hybrid enhancement ratio < 2. On the right, the red curves are for lower-hybrid enhancement ratio > 2. To the left, the red curves (lower-hybrid enhancement ratio < 2) are equal to, or slightly lower than, the black curves (all 6890 records). However, below 5 kHz, the red curves are significantly higher.

Note the following: On the left, the red curves pertain to ***low levels of lower-hybrid conversion of whistler waves***. On the right, the red curves pertain to ***high levels of lower-hybrid conversion***. Everywhere, the black curves are for all the records, regardless of lower-hybrid conversion.

The satellite perigee was ~400 km. Thus almost all of the recordings were taken either near the peak of the F-region, or in the topside ionosphere. None of these records sample the underside of the ionosphere. The nocturnal underside is still well above the Pederson layer (~140 km), so the underside ions are fully magnetized, thus fully capable of participating in lower-hybrid waves. At the reduced plasma densities of the underside, f_{lh} falls, and in the limit of low density, f_{lh} approaches f_{gi}, the ion plasma frequency. Thus the erosion of whistler energy at low frequencies (f < 7 kHz), shown to occur during periods of increased lower-hybrid activity, might be due to lower-hybrid conversion (scattering) on the F-region underside, well below the level of the satellite.